Novelty Journals

ISSN 2394-7349

International Journal of Novel Research in Engineering and Science
Vol. 9, Issue 2, pp: (1-12), Month: September 2022 - February 2023, Available at: www.noveltyjournals.com

INVESTIGATION OF MAGNETORESISTANCE OF CHEMICALLY SYNTHESIZED PAA/POLYANILINE/MWCNT NANOCOMPOSITE

Muktikanta Panigrahi[1*]

Materials Science, Maharaja Sriram Chandra Bhanja Deo University, 2nd Campus, Keonjhar-758002, Odisha, India

DOI: https://doi.org/10.5281/zenodo.7032011

Published Date: 1-September-2022

Abstract: **PAA/polyaniline/MWCNT nanocomposites are synthesised. Aniline is taken as monomer whereas; MWCNT is used as additive. Prepared nanocomposites are synthesized by chemical oxidation method. XRD, FTIR, and UV-Visible, FESEM with EDS, HRTEM, DC conductivity and magnetoresistance techniques are used to characterize the prepared nanocomposite as well as raw materials. Room temperature DC conductivity, temperature dependent (presence and absence magnetic field) of above-mentioned nanocomposites is estimated by linear four-probe technique. DC conductivity are found to be xxxx S/cm (of PAA/PANI/MWCNT (0.1 wt%) nanocomposites), xxx S/cm (of PAA/PANI/MWCNT (3 wt%) nanocomposites), xxx S/cm of PAA/PANI/MWCNT (0.3 wt%) nanocomposites. Magnetoresistance of PAA/PANI/MWCNT (0.5 wt%) nanocomposite, xxx S/cm (of PAA/PANI/MWCNT (1.0 wt%) nanocomposites) at room temperature. DC conductivity is a function of temperature. It is also studied with and without magnetic field. Conduction process of materials is followed Mott 3D-VRH model. Magnetoresistance (MR) is also estimated and shows positive MR.**

Keywords: **Acrylic Acid, Electrical Conductivity, Magnetoresistance, Mott 3D-VRH model, MWCNT , and Polyaniline.**

I. INTRODUCTION

In last decades, researchers/scientist are focused more attention on carbon nanotubes (CNT) based polymer nanocomposite. It is new class of multidirectional materials having improved mechanical, electrical, and thermal properties if compared with pure polymers [1-14]. Extensive reviews are studied on these CNT/polymer composite materials [1]. Nylon 6 composite fibers/SWCNT is prepared. Improved results is obtained by loading of SWCNT (0.5 wt %) [2]. SWCNT/poly (3-hexylthiophene) nanocomposite is prepared. From the results of as prepared material is characterized by electrical bistability and memory phenomenon. Single-walled CNT/polyurethane nanocomposites show strong microwave absorption (2-18 GHz) [3] Pradhan et al.3]. Aligned CNT based polymer composite films show high flexible, high transparency, and outstanding conductivity [5]. Polypyrrole with CNT based nanocomposite films is prepared. It shows better charge storage capacities. This is applied in supercapacitors and secondary batteries [6]. Prepared CNT loaded poly(3-octylthiophene) nanocomposite is tested (organic photovoltaic cells) and results is highly encouraging [7]. CNT loaded with polymer matrix. Nanocomposite is prepared by interfacial interactions between them and is indicated improved physical and chemical properties [1, 2, 8].

Mainly, magnetoresistance (MR) studies on polyaniline (PANI)/CNT nanocomposites and polypyrrole/CNT nanocomposites have been reported [12–14]. Temperature-dependent MR of this nanocomposite has not been reported [12-14]. Magnetoresistance at low temperature region explore hopping systems (e.g., CNT/conducting polymer nanocomposites). For doped semiconductors at low temperature region, Mott's theory is applicable [15–17]. On application of magnetic field orbit of a donor electron is shrieked. Hence, hopping integrals decreases. So, large positive MR (at sufficiently low temperatures) is generally expected for hopping process. This type of positive MR is found in inorganic and polymeric semiconductors [18-24].

In current work, preparation, morphology (surface and bulk) chracterization, DC conductivity in room temperature and low temperature (with and without magnetic field), and magnetoresistance of PAA/PANI/MWCNT nanocomposites is focused.

II. EXPERIMENTAL

MATERIALS

Multi-wall carbon nanotubes (MWCNT), acrylic acid, ammonium persulphate (APS) aniline, are used during preparation of PAA/PANI/MWCNT nanocomposite. All are 99% assay and synthetic grade except MWCNT. Acrylic acid, ammonium persulphate (APS) aniline are procured from Merck India. Distilled water is used. Purpose of using MWCNT is to improve conducting property.

PAA/PANI/MWCNT NANOCOMPOSITE(S) SYNTHESIS

Three PAA/PANI/MWCNT nanocomposites are synthesised. Chemical oxidation method is adopted to synthesize PAA/PANI/MWCNT nanocomposites [25, 26]. Two purposes are employed for taking Acrylic acid (AA). One is doping purpose. Other one is making PAA and it gives stability to the polyaniline. Appropriate amount AA is taken in requisite quantity of water and stirred continuously (for 15 minutes). Reaction is carried out at room temperature and is formed a colourless solution.

Liquid aniline (as monomer) is put on colourless acrylic acid solution and is made aniline solution. Furthermore, MWCNT is added on acrylic acid/aniline solution. Such solution is stirred continuously (for 1 h).

Ammonium persulphate (APS) is a water soluble oxidant. Such oxidant is participated (in solution form) to convert monomer to polymer. Freshly APS solution is prepared by taking 0.01 mol APS and 50 mL water.

Freshly APS solution is added through a funnel drop by drop (slowly) to the acrylic acid/aniline/MWCNT solution and stirred continuously (6 h) for completion of polymerization reaction. Polymerization color changes from colourless to deep green. Product is stayed to 12 h for completion of polymerization.

Polymerization product is filtered using Buckner funnel. It is washed with distilled water several times for getting colourless filtrate. It is dried under vacuum at 60 °C for 6 h to get desired materials (i.e., PAA/PANI/MWCNT nanocomposite). Two other PAA/PANI/MWCNT nanocomposites are synthesised in similar way.

III. CHARACTERIZATION METHODS

MICROSCOPY

Field emission scanning electron microscopy (FESEM) is showed by pallet samples. Before FESEM testing, pallet samples are dried at 60 ºC in a vacuum for 2 h. Gold coating is done by sputtering technique. Gold coated sample is placed in FESEM instrument. Name of FESEM instrument is Carl Zeiss Supra 40. Materials surface study is made by FESEM. FESEM instrument operating parameter is kept fixed i.e., operating voltage is to be 30 kV.

High resolution transmission electron microscopy (HRTEM) is essential to analysis bulk (i.e. inside) structure of microtone cutting samples. Such cutting samples are placed to carbon coated copper grid. LEICA Microsystem, GmBH, A-1170 instrument is employed to cut the test samples. JEM-2100 HRTEM, JEOL, Japan **HRTEM** instrument is used to do the HRTEM test. Internal structure, dispersion status, and amorphous or crystalline nature, of the prepared are made from the test.

Novelty Journals

ISSN 2394-7349

International Journal of Novel Research in Engineering and Science
Vol. 9, Issue 2, pp: (1-12), Month: September 2022 - February 2023, Available at: www.noveltyjournals.com

DC CONDUCTIVITY MEASUREMENT

DC-conductivity of as-prepared pallet samples is measured by linear four-probe fixing method. Test specimen is made contacts (i.e., four) with silver paste and is dried by air (for 1 h). Keithley 2400 programmable current source is employed to estimate conductivity. In four probe system, two terminal leads is allowed to pass a constant current from a current source. Inner two probes are measured voltage (*V*) across using a multimeter. Keithley 2000 digital multimeter is used to measure voltage. In four point-probe technique, resistivity (ρ) is calculated. For such calculation, expression **[**27**]** is as follows;

$$\rho = 2\pi S\left(\frac{V}{I}\right) \quad \text{.....} \qquad (1)$$

Where;

S is probe spacing in centimetres (cm). Probe spacing is constant

I is supplied current in milliamperes (*mA*)

Obtained voltage V is measured in millivolts (*mV*).

Conductivity (σ) is calculated and the relation is mentioned below;

$$\sigma = \frac{1}{\rho} \quad \text{.....(2)}$$

In addition, resistivity is measured with temperature variation. In two ways, temperature variation resistivity is determined with and without magnetic field. In both cases, resistivity measured using a linear four-probe technique. Highest room temperature resistivity PANI-ES/PAA/MWCNT nanocomposite sample is tested for low temperature resistivity measurement (with and without magnetic field). Temperature controller (Lake shore 331) is used. In low temperature resistivity measurement, a computer controlling measuring system is used. Keithley 220 programmable current source is allowed to pass current through two terminals probes and voltage (*V*) is measured two inner probes. For voltage measurement, a multimeter (2182 NANOVOLTAMETER Keithley) is used.

Magnetoresistance (MR) is investigated using a Helium Compressor (HC) (model HC-4E1)–sumitomo cryostat (model Ganis research CO, INC) equipped with 0.8T superconducting magnet (Lake shore electromagnet). Magnetoresistance (MR) measurements are performed (Upto 0.8 tesla). .

IV. RESULTS AND DISCUSSION

DC CONDUCTIVITY

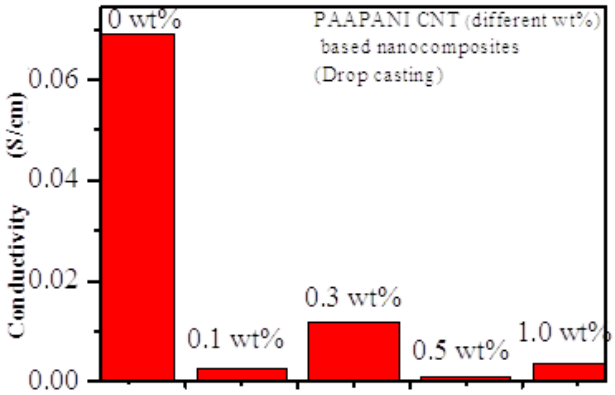

Figure 1 DC-Conductivity indicated materials

MWCNT is a good conductor of electricity [41,42] and also PANI has conductivity value. PAA is an insulator and have conductivity value. Both MWCNT and Acrylic acids are used for doping purpose as well as improve flexibility of conducting polyaniline. Acrylic acid is a weak dopant [28-30]. Medium of polymerization reaction is water (not inorganic acid solution). Therefore, DC-conductivity does not increase more. There is a bar diagram is plotted between DC-conductivity and MWCNT (wt%) (**Figure 1**). It displays a percolation threshold at a MWCNT (wt%) . Percolation effect indicates good dispersion of MWCNT in PAA/PANI/MWCNT nanocomposite system. **Figure 1** shows DC-Conductivity indicated materials i.e., PAA/PANI/MWCNT nanocomposite system. at lower concentration and at a 0.3 wt% MWCNT system shows highest DC conductivity value among MWCNT nanocomposite system [31].

Various reports of equivalent nanocomposite systems are available on lowering the DC conductivity [28-31]. In present work, DC conductivity is lower group in comparison of pure PAA/PANI composite. There is no particular reason for this lowering DC conductivity property.

It is believed that PAA is non-conducting and becomes supramolecularly linked with MWCNT ~~SG.~~ Because of the above reason, conducting paths decreases. This supramolecularly interacted ~~SG/PVA~~ PAA/PANI/MWCNT complex organizes into fibrils, dendrites or rods. So MWCNT is not dispersed properly in the composite system. Hence, PAA/PANI/MWCNT nanocomposite is found lower DC conductivity.

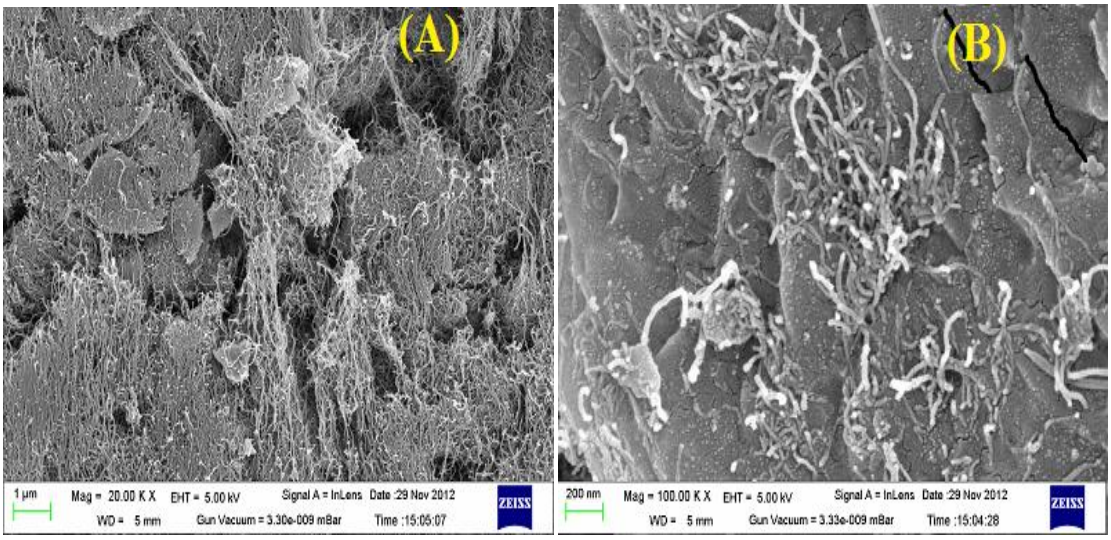

Figures 2 indicate FESEM morphology of polyaniline. It looks-like compacted closely tangled fibrillar morphology (Figure 2) with spaced. Figures 2A and 2B display FESEM images of MWCNT (lower magnification, A) and MWCNT (lower magnification, A). Figure 2A and 2B show tangled fiber-shaped morphologies. Its diameter ranges from 20-40 nm.

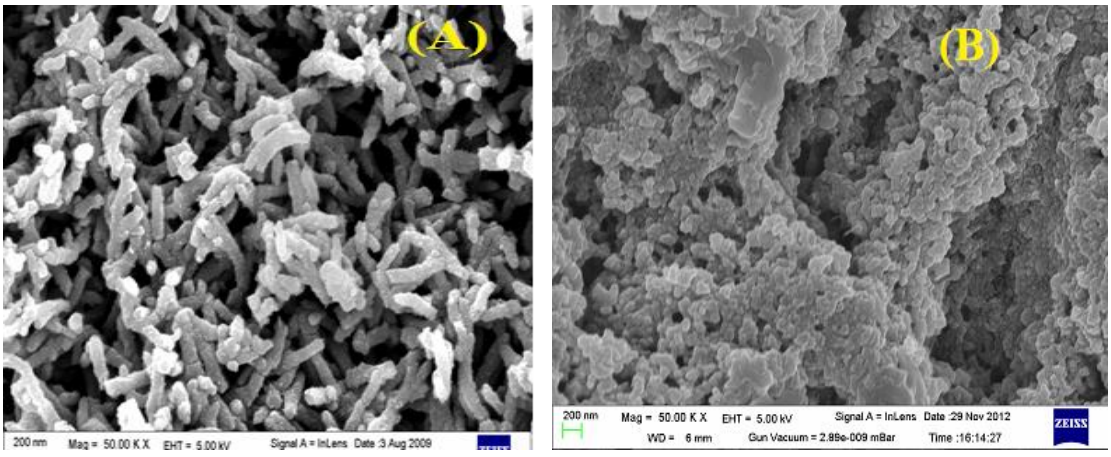

Figure 3 Pure PANI (A) and PAA/PANI-CNT (0.3%) nanocomposite (B)

Surface topography of PAA/PANI-CNT (0.3%) nanocomposite is shown in Figure 3(A and B). This image indicates compacted crystal. Crystals are connected to each other. This may happen due to bonding with dopant (Acrylic acid), MWCNT, PAA, and polyaniline. They are contributed in closering polyaniline Chains and it becomes higher ordered state. New morphology may arise due to self-organization of PAA/PANI/MWCNT (0.3 wt%). Self-organization is a type of supramolecular complex (PAA and PANI). Nature of supramolecular complex and its self-organization may depend on variation of interfacial interaction among them.

Figure 4A indicates HRTEM micrographs of MWCNT nanomaterial. Figure 4A looks-like entangled fibers. Diameter entangled fiber of MWCNT nanomaterial is found to be 20-40 nm. Figure 4B displays SAD partten of MWCNT nanomaterial. It shows equally spaced light-spots in a line. These spots are signified crystalline nature of MWCNT nanomaterial.

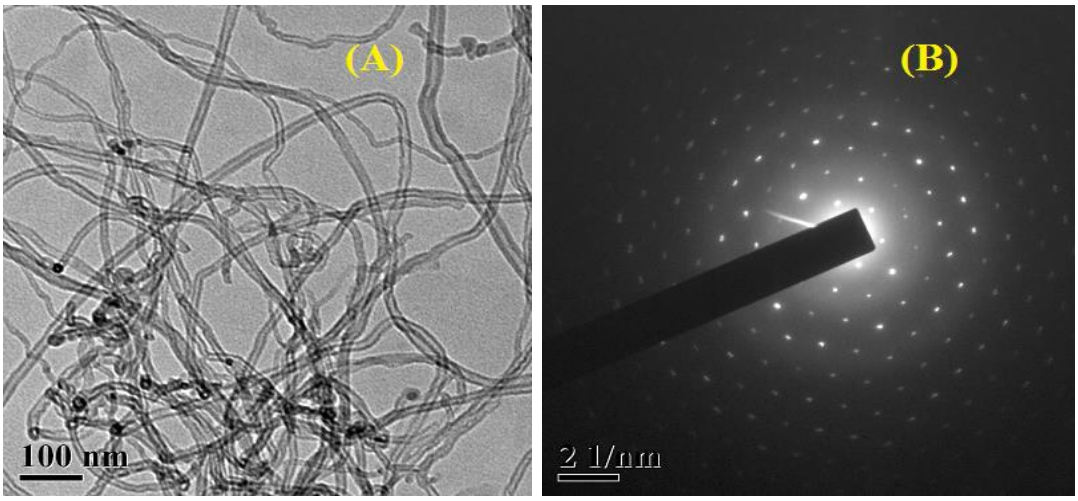

Figure 4 MWCNT image (A) and SAD parrten of MWCNT (B)

Bulk image is studied by TEM results analysis. Bulk image of PAA/PANI/MWCNT (0.3 wt%) nanocomposite is shown in Figure 5A. Entangled MWCNT nanomaterials are well dispersed in the PAA/PANI matrix.

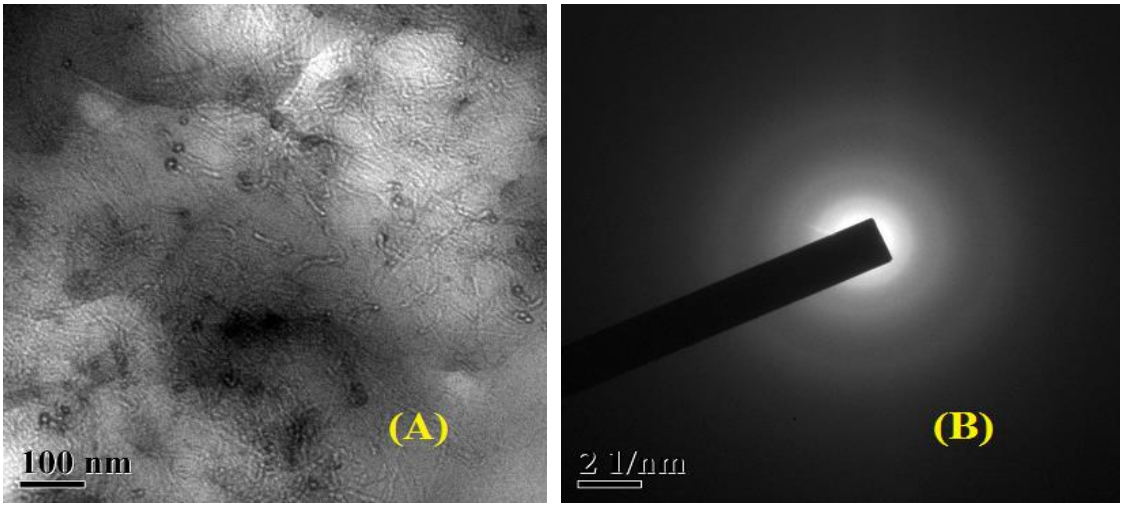

Figure 5 PAA/PANI/MWCNT (0.3 wt%) (A) and SAD pattern of PAA/PANI/MWCNT (0.3 wt %) (B)

SAD partten of PAA/PANI/MWCNT (0.3%) nanocomposite is shown in Figure 5B. There is not found equally spaced light-spots in a line in Figure 5B. Therefore, this SAD partten of PAA/PANI/MWCNT (0.3%) nanocomposite is signified amorphous nature. It may happen that MWCNT fibers enter into PAA/PANI inter-lamellar amorphous zone causing an increase of amorphous over layer thickness of PAA/PANI.

Novelty Journals

ISSN 2394-7349

International Journal of Novel Research in Engineering and Science
Vol. 9, Issue 2, pp: (1-12), Month: September 2022 - February 2023, Available at: www.noveltyjournals.com

TEMPERATURE DEPENDENT DC-CONDUCTIVITY

Temperature dependent DC resistivity of PAA/PANI/MWCNT nanocomposite is pointed in Figure 6 (Absence of magnetic field). Figure 6 shows resistivity is a function of temperature. On increasing temperature resistivity decreases (vide-Figure 6). Such nature is similar to the behaviour of inorganic semiconductor [25-27]. Hence, PAA/PANI-ES/MWCNT nanocomposite is called organic semiconductor [31]. This prepared materials show semiconducting behavior upto 300 K.

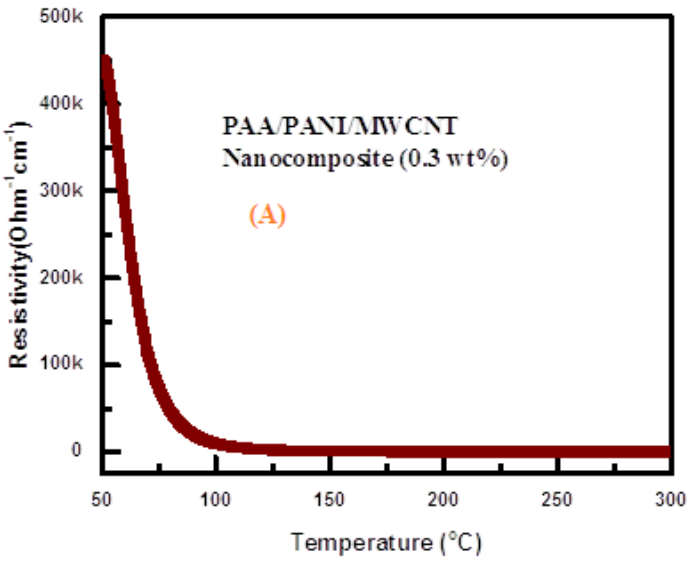

Figure 6 Temperature Dependent resistivity of indicated materials without field

It is clear that **for PAA/PANI/MWCNT** nanocomposite reveals semiconductor in the absence of magnetic field. Similar nature of **PAA/PANI/MWCNT** nanocomposite is observed from Figure 7 with field (at 0.8 Tesla). Resistance of **PAA/PANI/MWCNT** nanocomposite decreases upto 150 kelvin and then, it is saturated upto 300 kelvin (Figure 7). There is lowering resistance value in the presence of 0.8 tesla upto 150 kelvin. This lowering resistance may be happened due to presence of magnetic field. On increasing temperature, presence of electrons on the organic semiconductor (**PAA/PANI/MWCNT** nanocomposites) gains energy. Therefore, electrons jump from valency band to conduction band easily through Fermi level (upto 150 kelvin). Other aspect is gaining energy. There is possibility of scattering of moving electrons. Therefore, electron density is decreased. Hence, conductivity value decreases upto 150 kelvin. In the presence of magnetic field, all the electrons are conduction path. Hence, temperature dependent conductivity is more [].

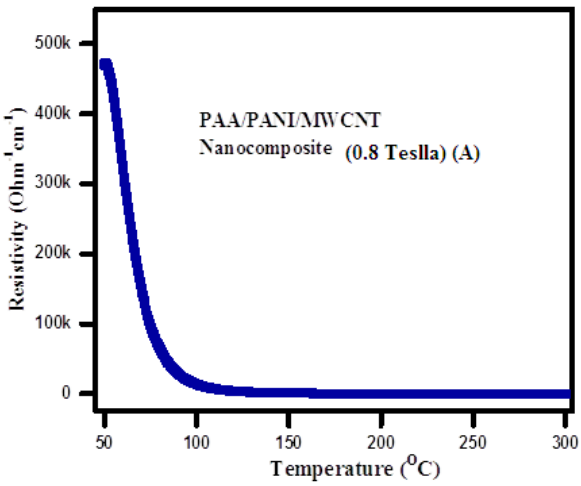

Figure 7 Temperature Dependent resistivity of indicated materials with field (0.8 Tesla)

Novelty Journals

ISSN 2394-7349

International Journal of Novel Research in Engineering and Science
Vol. 9, Issue 2, pp: (1-12), Month: September 2022 - February 2023, Available at: www.noveltyjournals.com

Variable range hoping (1D, 2D, 3D), Arrhenius model, etc are supported to understand conduction mechanism of conducting polymers. This study is made below room temperature i.e., 50 K to 300 K. 3D Mott's variable range hoping (Mott's VRH) model supports to hooping mechanism and is shown in Figure 8.. Arrhenius model is also plotted and is displayed in Figure 9. It explains the thermal activation process. Deciding factor is regression value. Regression value is obtained by linearly fitted plot.

$$\rho(T) = \rho_0 e^{\left(\frac{T_{Mott}}{T}\right)^{\frac{1}{4}}} \quad \text{.....(4)}$$

$$\sigma = \sigma_0 \exp\left(-\frac{T_0}{T}\right)^{r} \quad \text{.....(3)}$$

In Mott's 3D-VRH model, Graph is plotted between resistivity (ρ) and temperature range (50-300 K) and is fitted linearly using above equation [25-27]. T_0 is Mott characteristic temperature, whereas ρ_0 is limiting value of resistivity at infinite temperature. 'r' is dimensionality of transport process. Expression for dimensionality of transport process 'r' is as follows;

r=[1/(1+d)]

Here; d=1, 2 and 3 represent the one, two and three dimension, respectively. Figure xxxx shows Mott's 3D VRH plots.

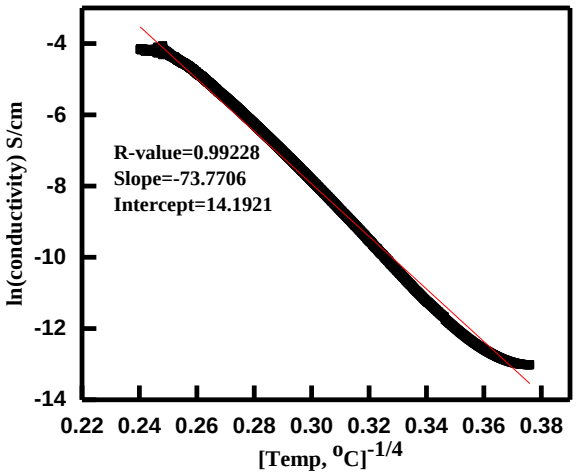

Figure 8 3D-VRH plot for PAA/PANI/MWCNT nanocomposite

Arrhenius model is used to determine activation energy. **Figure 9** shows the Arrhenius plot. Such graph is plotted between temperature ranges (in Kelvin scale) and logarithmic of DC conductivity. Arrhenius model is as follows; [27-30]

$$\sigma = \sigma_0 \exp\left(-\frac{E_a}{kT}\right) \quad \text{.....(5)}$$

Here; E_a is thermal activation energy and σ_a is a parameter which is obtained from Arrhenius model and is signified the semiconducting nature. Higher regression value (after linear fit) of Mott's 3D-VRH model and Arrhenius model obey the conduction process. Transport process is either Mott's VRH model or Arrhenius model [25-27]. Regression values (both Mott's 3D-VRH model and Arrhenius model) are mentioned in the Figures 8 and 9. From the above Figure xxx and xxx, it is clear that better regression value is obtained in Mott's 3D-VRH model (0.99856). Therefore, transport phenomenon follows Mott's 3D-VRH model [25-27]. So, charge carrier can hop both in between the chains, *i.e.*, interchain hopping and along the chain [25-27].

Novelty Journals

ISSN 2394-7349

International Journal of Novel Research in Engineering and Science
Vol. 9, Issue 2, pp: (1-12), Month: September 2022 - February 2023, Available at: www.noveltyjournals.com

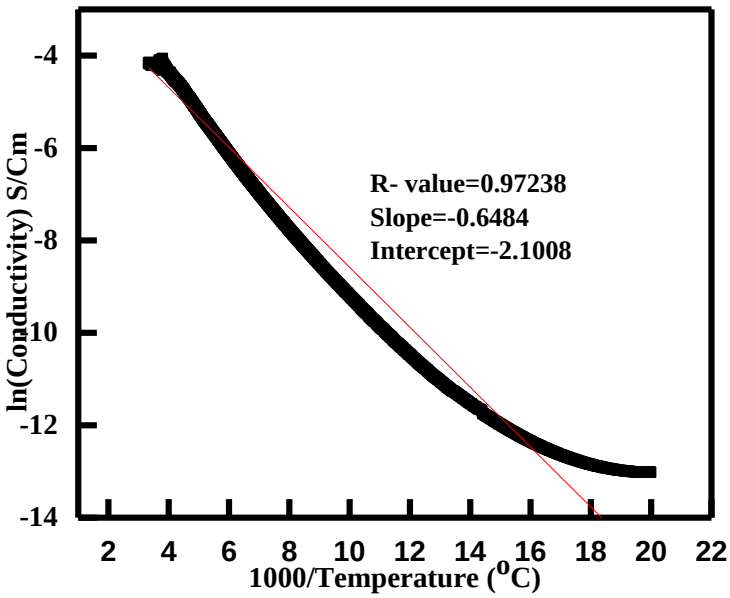

Figure 9 Arrhenius plot for PAA/PANI/MWCNT nanocomposite

In Mott 3D-VRH model, T_{mott} can be estimated from resistivity data among localized states and is described by following relation [25-30];

$$\rho(T) = \rho_0 e^{\left(\frac{T_{Mott}}{T}\right)^{\frac{1}{4}}} \quad \text{.....(6)}$$

$$T_{Mott} = \frac{16}{[K_B N(E)_F L^3_{loc}]} \quad \text{.....(7)}$$

Density of states at the Fermi level is determined by equation xxx

Here; K_B is Boltzmann constant

$N(E)_F$ is density of states at the Fermi level

L^3_{loc} is localization length

Localization length L_{loc} is estimated from temperature dependent conductivity at particular magnetic field (0.5 T) data (**Figure 10)** and expression is mentioned below [25-30]

$$\ln\left[\frac{\rho(H)}{\rho_0}\right] = t\,(L_{loc}/L_H)^4 \left(\frac{T_{Mott}}{T}\right)^{\frac{3}{4}} \quad \text{.....(8)}$$

Here; t = 5/2016,

L_H = magnetic length = $(hc/2\pi eH)^{1/2}$

c = velocity of light (3×10^{10} cm/s)

h = Planck's constant (6.62×10^{-27} erg.sec)

e = electronic charge (1.6×10^{-19} C)

Applied magnetic field (H) = 0.8 tesla (T)

Novelty Journals

ISSN 2394-7349

International Journal of Novel Research in Engineering and Science
Vol. 9, Issue 2, pp: (1-12), Month: September 2022 - February 2023, Available at: www.noveltyjournals.com

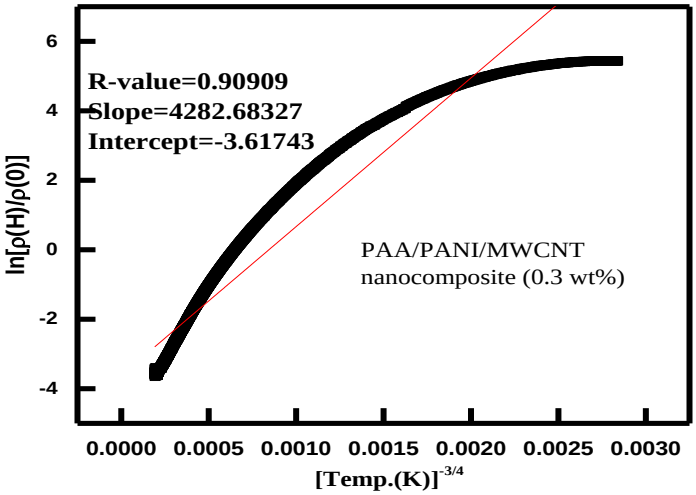

Figure 10 Plots of [ln ρ(H)/ρ(0)] *vs* $T^{-4/3}$ for PAA/PANI/MWCNT

Magnetoresistance (MR)

Magnetic Field dependent MR of results PAA/PANI/MWCNT nanocomposite (0.3wt %) is displayed in Figure 11 at different temperatures (i.e., 50K, 100K, 200K, and 300K). MR determined from 0.0 Gauss to 8.0 kilogauss. **Figure 11 A** shows MR of PAA/PANI/MWCNT nanocomposite (0.3wt %) **at 50 kelvin**. All cases, Magnetoresistance are magnetic field dependent. From 0.0 Gauss to 8.0 kilogauss, MR increases up to 1.0 kilogauss and then decreases (upto 8.0 kilogauss). Estimated MR (up to 8.0 gauss) is found to be positive for all 50K, 100K, 200K, and 300K. Figure 11B indicates MR decrease upto 4.0 kilogauss and then increases upto 8.0 kilogauss and MR values are positive. At 100 K, it shows metallic to the insulating regime (M-I) transition [31-45]. Figure 11C displays MR of PAA/PANI/MWCNT nanocomposite (0.3wt %) **at 200 kelvin.** It's MR value is positive. Figure 11D displays MR PAA/PANI/MWCNT nanocomposite (0.3wt %) **at 300 kelvin.** It's MR value is positive and is depended non-linearly.

Estimated positive MR value is due to influence of electron–electron interactions on low-temperature region and follows hopping conduction [31-45].

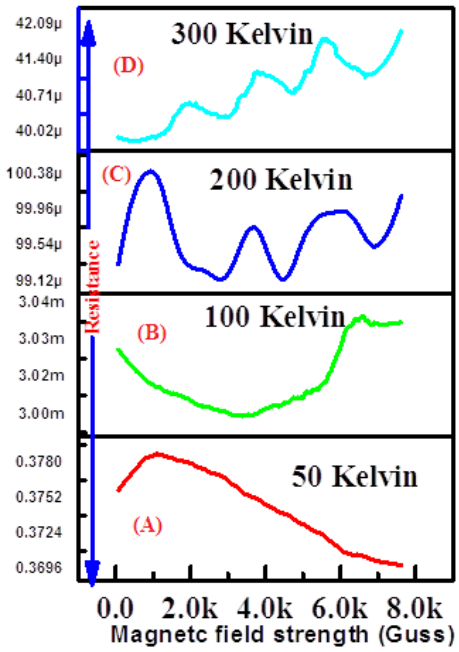

Figure 11 Magnetic field variation resistance at different temperature for PAA/PANI/MWCNT (0.3 wt%)

Positive MR is due to contraction of wave functions of electrons with increasing distance from the impurity center.15–17 This agrees to a large positive MR at low temperatures. 18. In high temperature regions, the positive MR value decreases due to increase overlap of wave functions of localized states.

V. CONCLUSIONS

PAA/PANI/MWCNT nanocomposite (0.3wt %) displays distinct morphology (surface and bulk) if compared with base material. This is due to supramolecular organization. Room temperature DC conductivity, Temperature variation DC resistivity, and Magnetic field dependent DC resistance of PAA/PANI/MWCNT nanocomposite (0.3wt %) are indicated. DC conductivity at room temperature decreases due to weak dopant and percolation effect. DC resistivity is a function of temperature. This results show three dimensional (3D) variable ranges hopping in conduction process. Magnetic field dependent resistance exhibits positive value of magnetic resistance. DC magnetic resistance studies in different temperatures (50 K, 100K, 200K, and 400K). More positive value of magnetic resistance founds in 50 kelvin temperature with variation of magnetic field (0.1 tesla to 0.8 tesla). Positive magnetic resistance value is due to shrinkage effect of wave function in hopping conduction mechanism.

In conclusion, such magnetoresistance Positive magnetic resistance value in PAA/PANI/MWCNT nanocomposite (0.3wt %) is controlled by a random network of inter-fibril structures.

ACKNOWLEDGMENTS

I acknowledge Prof Basudam Adhikari, Materials Science Centre for supporting the lab facility. I acknowledge CRF, Indian Institute of Technology, Kharagpur for supporting experimental works.

REFERENCES

[1] M. Moniruzzaman and K. I. Winey, Polymer nanocomposites containing carbon nanotubes, **Macromolecules**, **July 2006**, Vol. 39, Issue 16, pp. 5194-5205.

[2] J. Gao, B. Zhao, M. E. Itkis, E. Bekyarova, H. Hu, V. Kranak, A. Yu, and R. C. Haddon, Chemical engineering of the single-walled carbon nanotube−nylon 6 interface**, Journal of American Chemical Society, May 2006**, Vol. 128, Issue 23, pp. 7492-7496.

[3] B. Pradhan, S. K. Batabyal, and A. J. Pal, Electrical bistability and memory phenomenon in carbon nanotube-conjugated polymer matrixes, **Journal of Physical Chemistry B, April 2006**, Vol.. 110, Issue 16, pp. 8274-8277.

[4] Z. F. Liu, G. Bai, Y. Huang, F. F. Li, Y. F. Ma, T. Y. Guo, X. B. He, X. Lin, H. J. Gao, and Y. S. Chen, Microwave absorption of single-walled carbon nanotubes/soluble cross-linked polyurethane composites, **Journal of Physical Chemistry C, June 2007,** Vol. 111, Issue 37, pp13696-13700.

[5] H. Peng, Aligned Carbon nanotube/polymer composite films with robust flexibility, high transparency, and excellent conductivity, **Journal of American Chemical Society, Oct. 2008**, Vol. 130, Issue 1, pp.42-43.

[6] M. Hughes, M. S. P. Shaffer, A. C. Renouf, C. Singh, G. Z. Chen, D. J. Fray, and A. H. Windle, Electrochemical of nanocomposite films formed by coating aligned arrays of carbon nnotubes with polypyrrole, **Advanced Materials, Mar. 2002**, Vol. 14, Issue 5, pp. 382-385.

[7] E. Kymakis and G. A. Amaratunga, Single-wall carbon nanotube/conjugated polymer photovoltaic devices, **Journal of Applied Physical Letter, Jan. 2002**, Vol. 80, Issue 1, pp. 112-114.

[8] M. Yang, V. Koutsos, and M. Zaiser, Interactions between polymers and carbon nanotubes: a molecular dynamics study, **Journal of Physical Chemistry B, April 2005**, Vol. 109, Issue 20, pp. 10009-10014.

[9] J. N. Coleman, S. Curran, A. B. Dalton, A. P. Davey, B. McCarthy, W. Blau, and R. C. Barklie, Percolation-dominated conductivity in a conjugated-polymer-carbon-nanotube composite, **Physics Review B, Sep. 1998**, Vol. 58, Issue 12, R7492-R7495.

[10] G. B. Blanchet, C. R. Fincher, and F. Gao, Polyaniline nanotube composites: A high-resolution printable conductor, **Applied Physical Letter, Feb. 2003, V**ol. 82, Issue 8. Pp. 1290-1292.

[11] R. Ramasubramaniam, J. Chen, and H. Y. Liu, Homogeneous carbon nanotube/polymer composites for electrical applications, **Applied Physics Letters, Aug.2003**, Vol. 83, Issue 14, pp. 2928-2930.

[12] Y. Z. Long, Z. J. Chen, X. T. Zhang, J. Zhang, and Z. F. Liu, Synthesis and electrical properties of carbon nanotube polyaniline composites, **Applied Physics Letters, Jan 2004**, Vol. 85, Issue 10, pp. 1796-1798.

[13] Y. Long, Z. Chen, X. Zhang, J. Zhang and Z. Liu, Electrical properties of multi-walled carbon nanotube/polypyrrole nanocables: percolation-dominated conductivity**, Journal of Physics D: Applied Physics, June 2004.** Volume 37, Number 14

[14] X. Zhang, J. Zhang, R. Wang, and Z. Liu, Cationic surfactant directed polyaniline/CNT nanocables: synthesis, characterization, and enhanced electrical properties, **Carbon, Mar 2004**, Vol. 42, Issue 8-9, pp. 1455-1461.

[15] N. F. Mott and E. A. David, Electronic Processes in Noncrystalline Materials; Oxford University Press: Oxford, 1979; p 32.

[16] M. Pollak and B. I. Shklovskii, Hopping Transport in Solids; North-Holland: Amsterdam, 1991; p 273.

[17] B. I. Shklovskii and A. L. Efros, Electronic properties of doped semiconductors; Springer-Verlag: Berlin, 1984; p 202.

[18] T. Skotheim, R. Elsenbaumer, and J. Reynolds, Handbook of Conducting Polymers: Marcel Dekker: New York, 1998; pp. 27.

[19] A. K. Mukherjee and R. Menon, Magnetotransport in doped polyaniline, **Journal of Physics: Condensed Matter, Mar. 2005**, Vol. 17, Issue 12 , pp. 1947-xxx.

[20] Y. Long, Z. Chen, J. Shen, Z. Zhang, L. Zhang, K. Huang, M. Wan, A. Jin, C. Gu and J. L. Duvail, Magnetoresistance studies of polymer nanotube/wire pellets and single polymer nanotubes/wires, **Nanotechnology**, **Nov. 2006**, Vol. 17, Issue 24, pp. 5903-xxx.

[21] Y. Long, L. Zhang, Z. Chen, K. Huang, Y. Yang, H. Xiao, M. Wan, A. Jin, and C. Gu, Electronic transport in single polyaniline and polypyrrole microtubes**, Physical Reiview B, April 2005**, Vol. 71, issue 16, pp. 165412-7.

[22] A. Kurobe and H. Kamimura, Correlation effects on variable range hopping conduction and the magnetoresistance, **Journal of the Physical Society, Japan , Jan 1982**, Vol. 51, issue 6, pp. 1904-1913.

[23] V. L. Nguyen, B. Z. Spivak, and B. I. Shklovskii, Tunnel hopping in disordered systems, **Journal of Experimental and Theoretical Physics (JETP), Nov. 1985,** Vol. 62, issue 5, 1021-1029.

[24] U. Sivan, O. Entin-Wohlman, and Y. Imry, Orbital magnetoconductance in the variable-range–hopping regime, **Physical Review Letter, April 1988**, Vol. 60, issue 15, pp1566-1569.

[25] M. K. Panigrahi, and B. Adhikari, DL-Polylactide (Dl-PLA) based polyaniline composite for hydrogen gas sensors, ISBN: 9789390853403, DOI: 10.34256/ioriip2125, IOR INTERNATIONAL PRESS, 2021.

[26] M. K. Panigrahi, and B. Adhikari, Cloisite 20A based polyaniline nanocomposites for nitrogen dioxide (NO_2) gas sensors, ISBN: 9789390853403, DOI:10.34256/ioriip2123, IOR INTERNATIONAL PRESS, 2021.

[27] M. K. Panigrahi, S.B Majumdar, B. Adhikari, H_3PO_4–doped DL–PLA/PANI composite for methane gas sensing, **IEEE explorer, Dec. 2011**, Vol. 97, pp. 1−7.

[28] P. Chowdhury, B. Saha, B. Singha, S. Ghosh, and I. Basumallic, Effect of acrylic acid doping on the properties of chemically synthesized polyaniline, **Journal of the Indian Chemical Society, Feb. 2007**, Vol. 84, Issue 2, pp. 176-180.

[29] M. Singla, S. Awasthi, A. Srivastava, and D.V.S. Jain, Effect of doping of organic and inorganic acids on polyaniline/Mn 3O 4 composite for NTC and conductivity behaviour, **Sensors and Actuators A Physical, May 2007,** Vol. 136, Issue 2, pp. 604-612.

[30] M. Khalid,M. A. Tumelero, I. S. Brandt, V. C. Zoldan, J. J. S. Acuña, and A. A. Pasa, Electrical conductivity studies of polyaniline nanotubes doped with different sulfonic acids, **Indian Journal of Materials Science, Dec. 2013**, Vol. 2013, Issue xxx, pp.1-8.

[31] M. Sumita, K. Sakata, Y. Hayakawa, S. Asai, K. Miyasaka and M. Tanemura double percolation effect on the electrical conductivity of conductive particles filled polymer blends, **Colloid and Polymer Science**, **Feb. 1992**, Vol. 270, pp.134-139. .

[32] Y. W. Park, A. J. Heeger, M. A. Druy and A. G. MacDiarmid, Electrical transport in doped polyacetylene, **Journal of Chemical Physics, July 1980**, Vol. 73, issue 2, pp. 946–957.

[33] E. S. Choi, G. T. Kim, D. S. Suh, D. C. Kim, J. G. Park and Y. W. Park, Magnetoresistance of the metallic polyacetylene, **Synthetic Metal, Mar 1999**, issue 1,Vol. 100, pp. 3–12.

[34] D. S. Suh, T. J. Kim, A. N. Aleshin, Y. W. Park, G. Piao, K. Akagi, H. Shirakawa, J. S. Qualls, S. Y. Han and J. S. Brooks, Helical polyacetylene heavily doped with iodine: Magnetotransport, **The Journal of Chemical Physics, April 2001**, Vol. 114, issue 16, pp. 7222–7227.

[35] D. S. Suh, J. G. Park, J. S. Kim, D. C. Kim, T. J. Kim, A. N. Aleshin and Y. W. Park, Linear high-field magnetoconductivity of doped polyacetylene up to 30 Tesla, **Physical Review B: Condensed Matter Materials Physics, April 2002,** Vol. 65, issue 16, pp. 165210-5.

[36] V. I. Kozub, A. N. Aleshin, D. S. Suh and Y. W. Park, Evidence of magnetoresistance for nanojunction-controlled transport in heavily doped polyacetylene, **Physical Review B: Condensed Matter Materials Physics, 2002**, Vol. 65, issue 22, pp. 224204-5.

[37] R. Menon, C. O. Yoon, D. Moses, A. J. Heeger and Y. Cao, Transport in polyaniline near the critical regime of the metal-insulator transition, **Physical Review B: Condensed Matter, Dec. 1993**, Vol. 48, Issue 24,, pp. 17685-17694.

[38] O. Chauvet, S. Paschen, L. Forro, L. Zuppiroli, P. Bujard, K. Kai and W. Wernet, Magnetic and transport properties of polypyrrole doped with polyanions, **Synthetic Metal, Mar. 1994**, Vol. 63, issue 2, pp. 115-119.

[39] A. N. Aleshin, R. Kiebooms, R. Menon, F. Wudl and A. J. Heeger, Metallic conductivity at low temperatures in poly,,3,4-ethylenedioxythiophene… doped with PF6, **Physical Review B: Condensed Matter, Aug. 1997**, Vol. 56, Issue 7, pp. 3659-3663.

[40] A. N. Aleshin, S. R. Williams and A. J. Heeger, Transport properties of poly(3,4-ethylenedioxythiophene)/poly (styrenesulfonate**), Synthetic Metal, April 1998**, Vol. 94, iisue 2, pp.173–177.

[41] T. D. Nguyen, Y. Sheng, J. Rybicki, G. Veeraraghavan and M. Wohlgenannt, Magnetoresistance in π-conjugated organic sandwich devices with varying hyperfine and spin–orbit coupling strengths, and varying dopant concentrations, **Journal of Materials Chemistry, Feb. 2007**, Vol. 17, issue 19, pp. 1995-2001.

[42] O¨ . Mermer, G. Veeraraghavan, T. L. Francis, Y. Sheng, D. T. Nguyen, M. Wohlgenannt, A. Kohler, M. K. Al-Suti and M. S. Khan, Large magnetoresistance in nonmagnetic π-conjugated semiconductor thin film devices, **Physical Review B: Condensed Matter Materials Physics, Nov. 2005**, Vol. 72, issue 20, pp. 205202-12.

[43] V. N. Prigodin, J. D. Bergeson, D. M. Lincoln and A. J. Epstein, Anomalous room temperature magnetoresistance in organic semiconductors, **Synthetic Metal, May 2006**, Vol. 156, issue no. 9-10, pp. 757-761.

[44] R. Xu, A. Husmann, T. F. Rosenbaum, M. L. Saboungi, J. E. Enderby and P. B. Littlewood, Large magnetoresistance in non-magnetic silver chalcogenides**, Nature, 1997**, Vol. 390, issue 6655, pp. 57-60.

[45] C. L. Chien, F. Y. Yang, K. Liu, D. H. Reich and P. C. Searson, Very large magnetoresistance in electrodeposited single-crystal Bi thin films, **Journal of Applied Physics, April 2000**, Vol. 87, issue 9, pp. 4659-4664.